Thermochimica Acta 474 (2008) 57–61

Contents lists available at ScienceDirect

Thermochimica Acta

journal homepage: www.elsevier.com/locate/tca

Analysis of structural and magnetic phase transition behaviors of $La_{1-x}Sr_xCrO_3$ by measurement of heat capacity with thermal relaxation technique

Yuhta Matsunaga [a], Hitoshi Kawaji [b], Tooru Atake [b], Hiroki Takahashi [c], Takuya Hashimoto [a,*]

[a] Department of Integrated Sciences in Physics and Biology, College of Humanities and Sciences, Nihon University, 3-25-40 Sakurajousui, Setagaya-ku, Tokyo 156-8550, Japan
[b] Materials and Structures Laboratory, Tokyo Institute of Technology, 4259 Nagatsuta, Midori-ku, Yokohama 226-8503, Japan
[c] Department of Physics, College of Humanities and Sciences, Nihon University, 3-25-40 Sakurajousui, Setagaya-ku, Tokyo 156-8550, Japan

ARTICLE INFO

Article history:
Received 11 March 2008
Received in revised form 22 May 2008
Accepted 5 June 2008
Available online 14 June 2008

Keywords:
$La_{1-x}Sr_xCrO_3$
Heat capacity
Structural phase transition
Magnetic phase transition
Crystal structure

ABSTRACT

The heat capacity, C_p, of the $La_{1-x}Sr_xCrO_3$ system and its temperature dependence have been measured by a thermal relaxation technique. Both structural and magnetic phase transitions were detected at temperatures that can be surmised from the phase diagram proposed in previous studies. The observed variation in enthalpy after the first-order structural phase transition, ΔH, showed agreement with those measured by differential scanning calorimetry (DSC). A decrease in the variation in C_p in the second-order magnetic phase transition, ΔC_p, with an increase in Sr content was detected, which can be attributed to a decrease in electronic spin configuration entropy with an increase in Sr content. In the dependence of ΔC_p on Sr content, a bending point was also observed at $x \sim 0.12$, at which the crystal system varies from an orthorhombic-distorted perovskite structure to a rhombohedral-distorted perovskite structure.

1. Introduction

Oxides with a perovskite-type crystal structure including a 3d transition metal, $La_{1-x}Ae_xMO_3$ (Ae = Ca, Sr; M: 3d transition metal) show interesting property such as a high electrical conductivity at high temperatures in various gas atmospheres and a colossal magnetic resistance (CMR) [1–3]. The magnetic, electric and thermodynamic properties of $La_{1-x}Ae_xMO_3$ are affected by a slight distortion from the ideal cubic perovskite structure, which is often observed in most perovskite-type oxides. Therefore, clarifying the relationship between the precise crystal structure and the above-mentioned properties is essential for practical applications; however, the authors consider that there have been few exhaustive reports since oxygen non-stoichiometry, which should generate under some preparation conditions and is a factor affecting the crystal structure and properties, was not considered in most studies.

Among $La_{1-x}Ae_xMO_3$, $La_{1-x}Ae_xCrO_3$ prepared in O_2 or air is reported to have no oxygen deficiency regardless of Ae content, as determined from the results of thermogravimetry [4–6]. Thus, we regard that $La_{1-x}Ae_xCrO_3$ is the most suitable material for analyzing the relationship between crystal structure and various properties since distortion from the ideal cubic perovskite structure and chemical state of Cr, *i.e.*, the concentrations of holes and spins are determined only by Ae content. Moreover, the origin of the magnetic property of $La_{1-x}Ae_xCrO_3$ is the super-exchange interaction of magnetic spin on the t_{2g} orbital of the B site Cr ion. Because a similar super-exchange interaction of magnetic spin on an e_g orbital is proposed for $La_{1-x}Ae_xMnO_3$, which has been extensively studied as CMR materials, particularly at low Ae content, the analysis of the relationship between the crystal structure and magnetic property of $La_{1-x}Ae_xCrO_3$ might be the first step in elucidating the CMR mechanism of $La_{1-x}Ae_xMnO_3$.

In our previous study [7], we have analyzed the structural and magnetic phase transition of $La_{1-x}Sr_xCrO_3$ by differential scanning calorimetry (DSC), dilatometry, temperature-controlled X-ray diffraction analysis, and dc magnetic measurement using SQUID. Two types of phase transition, namely first-order structural phase transition from orthorhombic-distorted perovskite to rhombohedral-distorted perovskite and second-order phase transition from canted antiferromagnetic to paramagnetic, were observed. Phase transition temperature changed with Sr content, and we proposed a magnetic and structural phase diagram of $La_{1-x}Sr_xCrO_3$, which includes four phases: paramagnetic-orthorhombic, canted antiferromagnetic-orthorhombic, canted antiferromagnetic-rhombohedral, and paramagnetic-rhombohedral. In particular, we have measured the dependence of magnetization on external magnetic field at

* Corresponding author. Tel.: +81 3 3329 1151x5516; fax: +81 3 5317 9432.
E-mail address: takuya@chs.nihon-u.ac.jp (T. Hashimoto).

0040-6031/$ – see front matter © 2008 Elsevier B.V. All rights reserved.
doi:10.1016/j.tca.2008.06.005

various temperatures for specimens with an Sr content x higher than 0.12 [8]. It has been revealed that the residual magnetization and coercive force of canted antiferromagnetic phase are affected by the first-order structural phase transition.

According to the phase diagram previously proposed [7], two types of second-order phase transition from a canted antiferromagnetic phase to a paramagnetic phase are shown: one is observed in the phase of orthorhombic-distorted perovskite for specimens with x lower than 0.12, whereas the other is detected in rhombohedral-distorted perovskite for specimens with x higher than 0.12. It is probable that behavior of the second-order phase transition varies depending on crystal structure. However, even the direct measurement of heat capacity (C_p), the most fundamental thermodynamic property, has not been carried out for $La_{1-x}Sr_xCrO_3$ and its variation in the second-order phase transition, ΔC_p, has not been sufficiently estimated.

In this study, the C_p of $La_{1-x}Sr_xCrO_3$ below room temperature has been measured using a thermal relaxation technique. The evaluated C_p and observed phase transition behavior have been compared with the results observed by DSC and dc magnetic measurement. The effect of the crystal system on ΔC_p has been investigated for the first time.

2. Experimental

Polycrystalline specimens of $La_{1-x}Sr_xCrO_3$ ($x = 0.00$–0.25) were prepared by the Pechini method [9]. Details of the preparation process are the same as those previously reported [7]. For powder X-ray diffraction analysis (Cu Kα; 50 kV, 250 mA, Rigaku RINT-2500) and differential scanning calorimetry (DSC; DSC8230, Rigaku Co., Ltd.), some of the obtained $La_{1-x}Sr_xCrO_3$ pellets were reground into powder in an alumina mortar. X-ray diffraction analysis at room temperature indicated that the obtained specimens were single-phase orthorhombic-distorted perovskite and rhombohedral one with $x < 0.10$ and $x > 0.10$, respectively. For $La_{0.9}Sr_{0.1}CrO_3$, a mixture of the two phases was obtained [10]. DSC was carried out by a method that is completely same as the previously reported one [7].

The dc magnetic susceptibility of the sintered $La_{1-x}Sr_xCrO_3$ was measured with a SQUID magnetometer (Quantum Design Inc., MPMS model). The temperature of the sample was controlled to be at measurement level after zero magnetic field cooling (ZFC) and then magnetic susceptibility was measured under an external magnetic field of 2 kOe. The measurement temperature range was 2.2–300 K at a heating rate of 1 K/min.

For C_p measurement, sintered $La_{1-x}Sr_xCrO_3$ pellets were shaped into rectangular form of about 2.0 mm × 2.0 mm × 1.0 mm. The C_p of the thus-shaped specimens were measured using PPMS (Physical Property measurement system; Quantum Design Inc.) with a heat capacity option by a thermal relaxation technique of the step scanning method under vacuum with a temperature range of 1.8–310 K.

3. Results

Fig. 1 shows the temperature dependence of the C_p of $La_{1-x}Sr_xCrO_3$. A heat capacity jump was observed for every $La_{1-x}Sr_xCrO_3$ as depicted by downward arrows. The temperature, at which the heat capacity jump was observed, decreased with an increase in Sr content. Fig. 2 shows the temperature dependence of the reciprocal of dc magnetic susceptibility, χ^{-1}, of $La_{1-x}Sr_xCrO_3$. A discrete increase in χ^{-1} was observed at temperatures depicted by upward arrows. Linear relationships were detected above the temperature as shown in dotted lines, indicating a paramagnetic

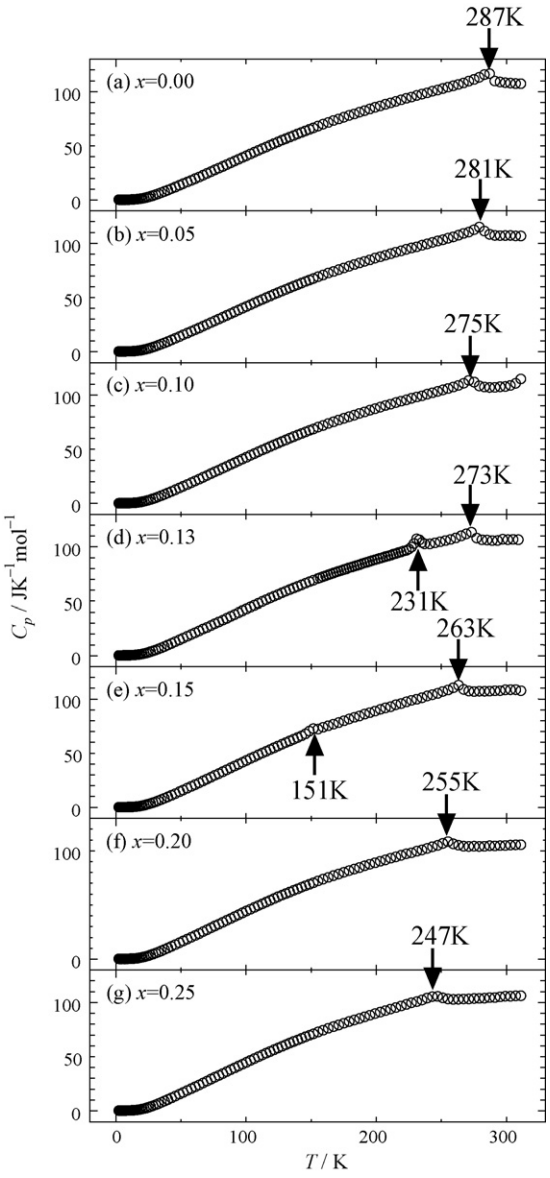

Fig. 1. Heat capacities of $La_{1-x}Sr_xCrO_3$: (a) $x = 0.00$, (b) $x = 0.05$, (c) $x = 0.10$, (d) $x = 0.13$, (e) $x = 0.15$, (f) $x = 0.20$, and (g) $x = 0.25$ measured by thermal relaxation technique. Heat capacity jumps originating from the second-order magnetic phase transition are denoted by downward arrows. The peaks due to the first-order structural phase transition are represented by upward arrows.

property that obeys the Curie–Weiss law. The small χ^{-1}, *i.e.*, the large χ below the temperature suggested a canted antiferromagnetic property, which was confirmed from the dependence of magnetization on external magnetic field [7,8]. Since the temperatures denoted by upward arrows in Fig. 2 agreed, the heat capacity jump depicted by downward arrows in Fig. 1 can be ascribed to the second-order magnetic phase transition. This phase transition has also been detected in DSC curves as a baseline shift, as shown in Fig. 3 and Ref. [7]. A smaller baseline shift was observed with an increase in Sr content, showing correspondence with the smaller ΔC_p in the specimens with higher Sr content, which will be discussed later.

For the specimens with $x = 0.13$ and 0.15, additional peaks were detected at 231 K and 151 K, respectively, from the temperature dependence of C_p as shown in Fig. 1(d) and (e). These temper-

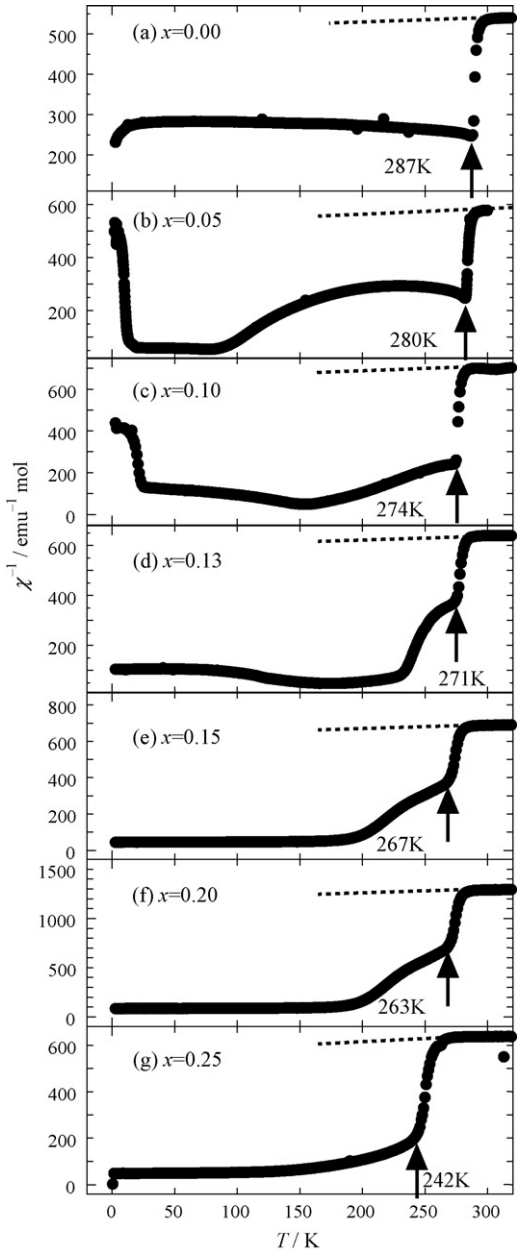

Fig. 2. Temperature dependence of reciprocal of DC magnetic susceptibility of $La_{1-x}Sr_xCrO_3$ measured at 2 kOe. The discrete increase indicating magnetic phase transition is shown by upward arrows.

atures corresponded to those at which endothermic peaks were observed in the DSC curves in Fig. 3(b) and (c), respectively. X-ray diffraction analysis at low temperatures revealed that the endothermic peak of DSC originated from the first-order structural phase transition from orthorhombic-distorted perovskite to rhombohedral-distorted perovskite [7]. Thus, it can be concluded that the first-order structural phase transition of the $La_{1-x}Sr_xCrO_3$ system can be successfully detected by a thermal relaxation technique although it has frequently been reported that this method is not suitable for the detection of the first-order phase transition. The reason for the successful detection and non-detection of the C_p peak in the other specimens will be discussed in the next section.

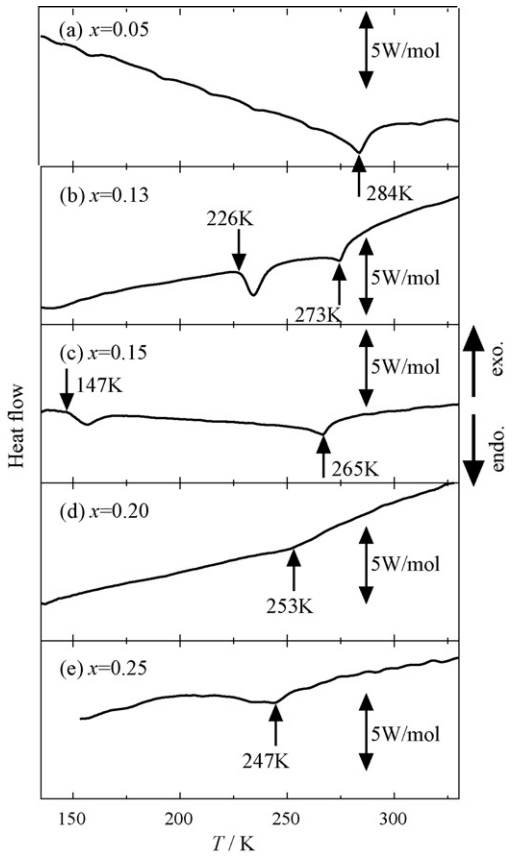

Fig. 3. DSC curves of $La_{1-x}Sr_xCrO_3$: (a) $x = 0.05$, (b) $x = 0.13$, (c) $x = 0.15$, (d) $x = 0.20$, and (e) $x = 0.25$. The baseline shifts are indicated by upward arrows and endothermic peaks are indicated by downward arrows.

4. Discussion

4.1. Effect of first-order structural phase transition on C_p

Essentially, no latent heat of the first-order phase transition can be detected by a thermal relaxation technique because of the irreversibility of the first-order phase transition, *i.e.*, thermal hysterisis. Fig. 4 shows the DSC curves of $LaCrO_3$ and $La_{0.95}Sr_{0.05}CrO_3$ during

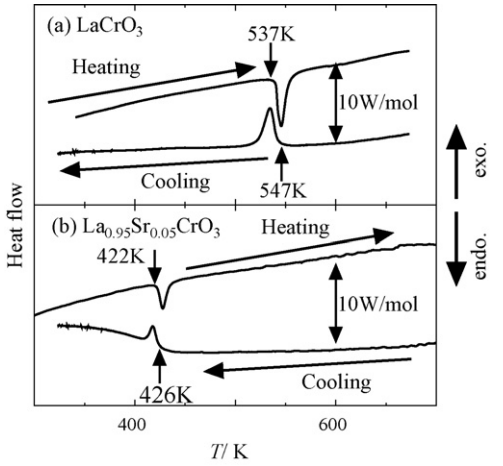

Fig. 4. DSC curves of (a) $LaCrO_3$ and (b) $La_{0.95}Sr_{0.05}CrO_3$ during heating and cooling procedures. The endothermic peaks during heating and the exothermic peaks during cooling are represented by downward and upward arrows, respectively.

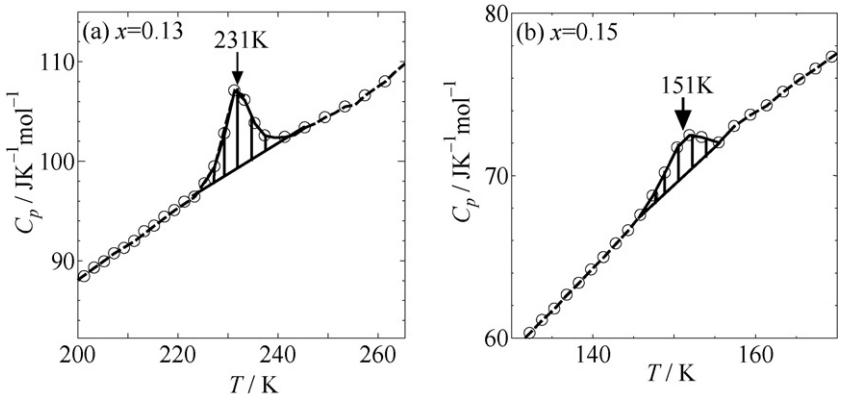

Fig. 5. Heat capacities of (a) $La_{0.87}Sr_{0.13}CrO_3$ at approximately 231 K and of (b) $La_{0.85}Sr_{0.15}CrO_3$ at approximately 151 K measured by thermal relaxation technique. The ΔHs for $La_{0.87}Sr_{0.13}CrO_3$ and $La_{0.85}Sr_{0.15}CrO_3$ were estimated from the hatched peak area.

the heating and cooling procedure. It can be concluded that the structural phase transition in both specimens is reversible since both the endothermic peak on heating and the exothermic peak on cooling were observed at almost the same temperatures and the variation in enthalpy in the first-order phase transition, ΔH, were almost the same. We regard that the first-order structural phase transition in $La_{1-x}Sr_xCrO_3$ could be successfully detected by the thermal relaxation technique owing to this reversibility.

For $La_{0.87}Sr_{0.13}CrO_3$ and $La_{0.85}Sr_{0.15}CrO_3$, ΔH can be estimated from the peak area detected in the temperature dependence of C_p enlarged in Fig. 5. The calculated ΔHs are plotted in Fig. 6. Fig. 6 also shows the ΔH calculated from the endothermic peak area observed by DSC [7]. ΔH measured by both methods showed good agreement. Since ΔH decreases with Sr content, it can be concluded that the non-observation of the peak identified as the first-order phase transition for specimens with x larger than 0.20 is due to a small ΔH. For the specimens with $x = 0.00$–0.10, the temperature of the first-order phase transition is too high to be detected by the thermal relaxation technique.

4.2. Effect of crystal structure on ΔC_p

Because of difficulty in settling baseline for the temperature dependence of C_p, the estimation of the entropy of the $La_{1-x}Sr_xCrO_3$ system is difficult. Therefore, we employ ΔC_p as a parameter for describing the behavior of the second-order phase transition instead of entropy. We regard that this assumption is highly applicable since the variation in the second-order phase transition temperature with Sr content is sufficiently small. Fig. 7 shows the ΔC_p evaluated from Fig. 1. ΔC_p decreases with an increase in Sr content with a bending point at $x \sim 0.12$, where the crystal structure changes. It can be considered that the ΔC_p of the specimens with x larger than 0.20 is so small that no baseline shift in the second-order phase transition is observed in the DSC curves, as shown in Fig. 3(d) and (e).

Since the electronic configuration of Cr^{3+} in $LaCrO_3$ is $3d^3$, electronic spin configurational entropy will be expressed as Rln4. In the second-order phase transition where a canted antiferromagnetic phase transforms to a paramagnetic phase, ΔC_p corresponding to the entropy of the electronic spin configuration should be observed. With Sr^{2+} substitution for the La^{3+} site, holes should be generated in the electronic band mainly composed of Cr 3d orbitals, resulting in a decrease in the concentration of electrons. Therefore, it can be surmised that electronic spin configurational entropy decreases with an increase in Sr content, resulting in a decrease in ΔC_p, which is shown in Fig. 7. However, the bending point observed at $x \sim 0.12$ cannot be explained in this discussion considering only the electronic spin configuration.

The variation in ΔC_p with Sr content represented by the dashed line in Fig. 7 could be expected if the crystal system of specimens

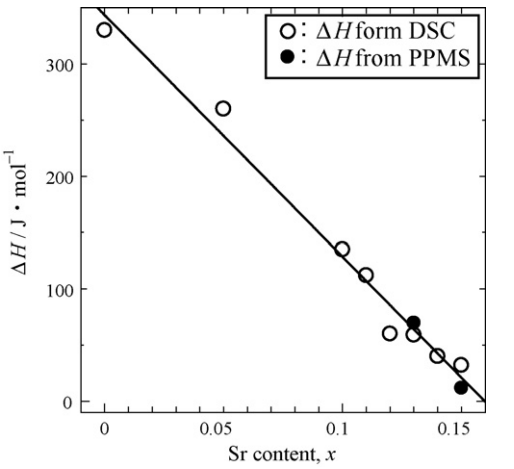

Fig. 6. Variation in enthalpy after first-order phase transition (ΔH) of $La_{1-x}Sr_xCrO_3$ ($x = 0.00$–0.25). ΔHs were calculated from the endothermic peak area of the DSC curves (○, [7]) and from the temperature dependence of heat capacity measured by the thermal relaxation technique (●).

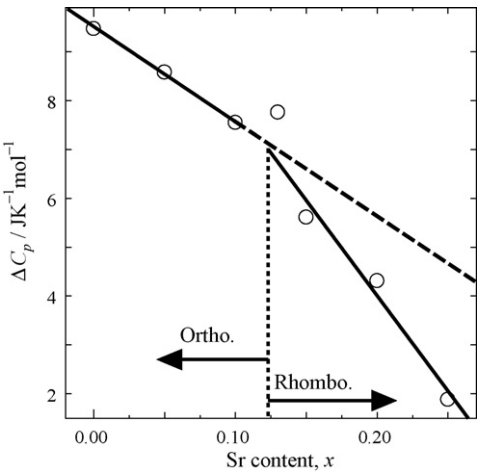

Fig. 7. Variation in ΔC_p after second-order phase transition of $La_{1-x}Sr_xCrO_3$ with Sr content x. The dashed line is the extrapolation of ΔC_p from the orthorhombic phase.

with x larger than 0.13 was orthorhombic; it was observed that the amount of decrease in ΔC_p in the rhombohedoral phase was larger than that in the orthorhombic phase. Thus, it can be concluded that not only a decrease in electronic spin configuration entropy with Sr substitution but also a slight variation in crystal structure affects ΔC_p, the mechanism of which is being investigated at present.

5. Conclusion

Both the first-order structural and second-order magnetic phase transitions in the $La_{1-x}Sr_xCrO_3$ system can be successfully detected by heat capacity measurement using a thermal relaxation technique. The observed phase transition temperatures agreed well with those detected by other methods such as DSC and dc susceptibility measurement. The ΔH in the first-order phase transition observed in this study showed agreement with those evaluated by DSC, and even small ΔHs in $La_{0.87}Sr_{0.13}CrO_3$ and $La_{0.85}Sr_{0.15}CrO_3$ can be successfully estimated by this method. Also clarified was the decrease in ΔC_p with an increase in Sr content with the bending point at $x \sim 0.12$. It is surmised that the decrease in ΔC_p with Sr content is due to a decrease in electronic spin configuration entropy with an increase in Sr content and that the bending point can be attributed to the variation in crystal structure, whose mechanism is now being investigated.

References

[1] N.Q. Minh, J. Am. Ceram. Soc. 76 (1993) 563.
[2] N. Sakai, H. Fjellvåg, B.C. Hauback, J. Solid State Chem. 121 (1996) 202.
[3] Y. Tokura, A. Urushubara, Y. Moritomo, T. Arima, A. Asamitsu, G. Kido, N. Furukawa, J. Phys. Soc. Jpn. 63 (1994) 3931.
[4] S. Onuma, K. Yashiro, S. Miyoshi, A. Kaimai, H. Matsumoto, Y. Nigara, T. Kawada, J. Mizusaki, K. Kawamura, N. Sakai, H. Yokokawa, Solid State Ionics 174 (2004) 287.
[5] T. Nakamura, G. Petzow, L.J. Gauckler, Mater. Res. Bull. 14 (1979) 649.
[6] J. Mizusaki, S. Yamauchi, K. Fueki, A. Ishikawa, Solid State Ionics 12 (1987) 119.
[7] F. Nakamura, Y. Matsunaga, N. Ohba, K. Arai, H. Matsubara, H. Takahashi, T. Hashimoto, Thermochim. Acta 435 (2005) 222.
[8] Y. Matsunaga, F. Nakamura, H. Takahashi, T. Hashimoto, Solid State Commun. 145 (2008) 502.
[9] M.P. Pechini, US Patent 3,330 (1967) 697.
[10] A. Mitsui, K. Homma, Y. Kumekawa, F. Nakamura, N. Ohba, Y. Hoshino, T. Hashimoto, J. Electrochem. Soc. 155 (2008) A395.